Available online at www.sciencedirect.com
ScienceDirect
International Journal of Heat and Mass Transfer 50 (2007) 3490–3497
International Journal of HEAT and MASS TRANSFER
www.elsevier.com/locate/ijhmt

Effect of gravity on cryogenic boiling heat transfer during tube quenching

Osamu Kawanami [a,*], Hisao Azuma [b], Haruhiko Ohta [c]

[a] Department of Mechanical System and Engineering, University of Hyogo, 2167 Shosha, Himeji, Hyogo 671-2201, Japan
[b] Department of Aerospace Engineering, Osaka Prefecture University, 1-1 Gakuen-cho, Sakai, Osaka 599-8531, Japan
[c] Department of Aeronautics and Astronautics, Kyushu University, 744 Motooka, Nishi-ku, Fukuoka 819-0395, Japan

Received 21 June 2006; received in revised form 14 December 2006
Available online 6 April 2007

Abstract

Cryogenic forced convective boiling under terrestrial and microgravity conditions for the development of cryogenic fluid management on orbit is studied. The experiments are conducted in a low mass velocity region (100–300 kg/m^2 s) that is easily influenced by gravity, and fluid behavior observations and heat transfer measurements are performed simultaneously. These experiments aim at understanding the effect of gravitational acceleration on the relation between the flow behavior and thermal characteristics during the quenching of the tube by a cryogenic fluid. The heat transfer increases under microgravity conditions, and results from an increase in the quench front velocity.

Keywords: Cryogenics; Forced convective boiling; Microgravity; Heat transfer

1. Introduction

During the re-ignition of a rocket engine in space, when a small amount of the residual propellant is transferred from the tank to the combustion chamber, it is important to precisely understand whether the phenomena that occur in space differ from those on the ground [1]. In addition to this, cryogenic propellants such as liquid hydrogen, liquid oxygen and liquid helium will require to be managed on orbit for future space transportation systems such as a system for fuel resupply on orbit [2]. Cryogenic fluid management on orbit is an area of technology that will be common to all future space missions [3].

To clarify the effects of gravity on heat transfer during tube quenching by cryogenic fluids, we investigated cryogenic forced convective boiling under microgravity conditions. Microgravity flow boiling, unlike pool boiling [4] and adiabatic two-phase flow, has not received significant attention in the past. In particular, experiments on cryogenic flow boiling in microgravity have hardly been conducted to date. This is due to the fact that this is by far the most difficult and complex boiling experiments [5]. To our knowledge, only one other experimental report, that by Antar and Collins [6], deals with this subject. They investigated flow patterns and heat transfer during a quenching process using a NASA KC-135 aircraft. They employed a quartz tube with an ID of 1.05 cm and a stainless tube with an ID of 0.432 cm for the visual recording of the flow patterns and measurement of the outer wall temperature, respectively. However, these experiments did not report the heat transfer characteristics of the quenching process, such as the heat flux and heat transfer coefficient. In addition, the terrestrial and microgravity experiments were generally not conducted under the same mass velocity condition. Hence, the heat transfer characteristics of cryogenic flow boiling during tube quenching in microgravity need to be studied further.

Here, we present the results of our microgravity experiments. These experiments were conducted at the Japan

* Corresponding author. Tel./fax: +81 79 267 4844.
E-mail address: kawanami@eng.u-hyogo.ac.jp (O. Kawanami).

0017-9310/$ - see front matter © 2007 Elsevier Ltd. All rights reserved.
doi:10.1016/j.ijheatmasstransfer.2007.01.025

Nomenclature

g_0	normal gravity acceleration (=9.8 m/s^2)	z	coordinate of axial direction (m)
1g	terrestrial conditions	ID	inner diameter of the tube
μg	microgravity conditions		
G	mass velocity (kg/m^2 s)	*Greek symbols*	
T	temperature (K)	α	heat transfer coefficient (W/m^2 K)
R	resistance (Ω)	ρ	density of the tube (kg/m^3)
u_q	quench front velocity (m/s)	κ	thermal conductivity of the tube (W/mK)
u_I	liquid velocity at the inlet of the test section (m/s)	δ	tube wall thickness (m)
q	heat flux (W/m^2)	*Subscripts*	
q_G	heat generated by the gold film (W/m^2)	l	liquid
c_p	specific heat of the tube (J/kg K)	w	inner wall of the tube
r	coordinate of radial direction (m)		

Microgravity Center (JAMIC) from 1999 to 2002, and were specifically aimed at understanding the heat transfer characteristics and flow pattern during the quenching of a tube in ambient conditions using liquid nitrogen as the test fluid.

2. Experimental apparatus and procedure

2.1. Experimental apparatus

A schematic diagram of the experimental apparatus used in this study is shown in Fig. 1, and a detailed drawing of the test section is given in Fig. 2. For safety considerations, LN_2 is selected as the test fluid in the present experiments; in addition, LN_2 is a suitable model fluid, because its surface tension, boiling point and evaporative latent heat are similar to liquid oxygen and liquid hydrogen comparatively well. The apparatus mainly consists of the test section, LN_2 and GN_2 tanks, air compressor (HITACHI BEBICON 0.2LP-7S), vacuum pump (ULVAC DA-15D), data logger (HP 34970A), and 2-set CCD cameras (TOSHIBA IK-M40). The test configuration is made to fit within a 425 × 870× 918 mm^3 frame at the JAMIC. The same apparatus is used in both the terrestrial tests and microgravity tests.

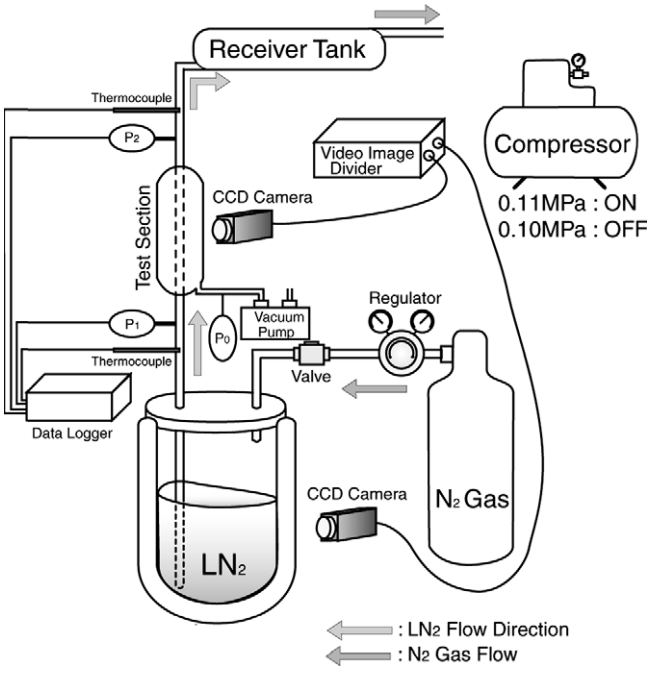

Fig. 1. Schematic diagram of the flow configuration used in the microgravity experiment.

The test section consists of a transparent heated tube [7], that is surrounded by vacuum insulation and is vertically oriented under terrestrial conditions. The tube is made of pyrex glass, and it has an ID of 7 mm and a wall thickness of 1 mm. The temperature measurement length is approximately 50 mm, and its inner wall is uniformly coated with a transparent gold film with a thickness of the order of 0.01 μm. The film is used as a resistance thermometer to directly evaluate the inner wall temperature averaged over the entire temperature measurement length. In this study, the thermostatic bath was used to examine the relationship between a resistance of the film and its temperature. Additionally, the transparency of the film allows visual observation of the flow behavior through the wall. Both ends of the tube are coated with a thick layer of silver film for use as electrodes and are in contact with a brass flange, as shown in Fig. 2. Several ring sheets made of aluminum foil are inserted between the tube and brass flanges to remove additional electrical resistances and prevent thermal deformation. The brass flanges are used for power supply and to seal the tubes with O-rings. The upstream and downstream ends of the copper tube serve as the entrance and exit sections, respectively. The length of the copper tube is decided as the maximum allowable length restricted by the apparatus height in the microgravity facility employed. The LN_2 reservoir tank is located directly below the test section. The passage exit is opened to the outside.

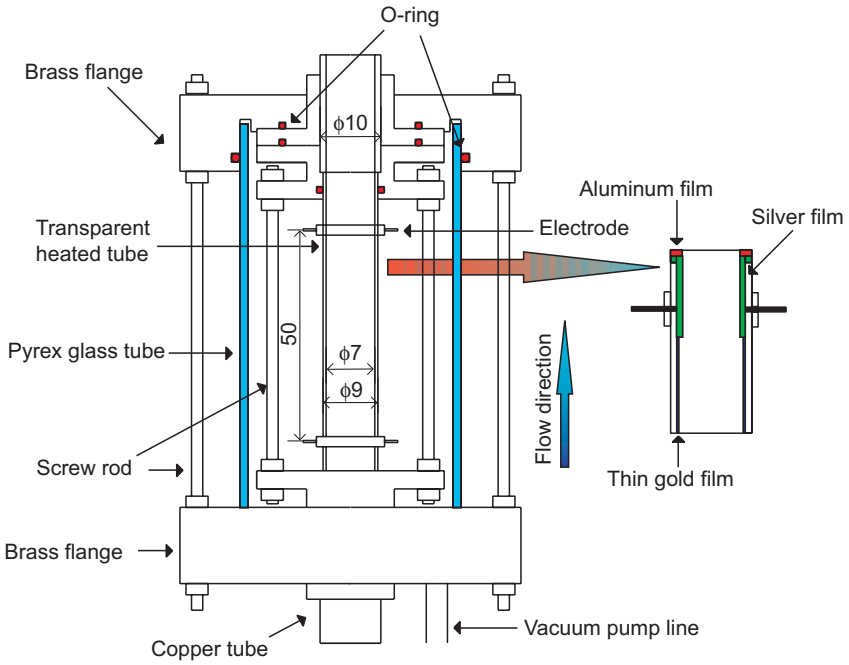

Fig. 2. Detailed view of the test section with the transparent heated tube.

2.2. Outline of the drop shaft experiments

The Japan Microgravity Center (JAMIC) had a drop shaft located at Kamisunagawa, Hokkaido (currently inoperative). The drop shaft was the largest in the world, with a free fall section of approximately 500 m, and was capable of producing a microgravity environment with a duration of about 10 s [8]. An experimental capsule that is dropped in the free fall section consists of a thruster module, a payload module, and a bus module with the coordinate axes. In order to compensate for the air drag on the capsule during free fall, the position of the outer capsule can be roughly compensated by thrusting gas from the thruster module. The space between the inner capsule (where the experimental apparatus is installed) and the outer one (the payload module) is evacuated, so that the inner capsule is not affected by air drag during free fall. The free space in the entire experimental apparatus in the inner capsule is 0.87 m (W) × 0.87 m (D) × 0.90 m (H), with a maximum payload weight of 500 kg. We used half (0.425 m width) of this space.

A typical example of the variation in the gravity level during the drop shaft experiments is shown in Fig. 3. After the capsule is released, the magnitude of the z-axis acceleration (referred to as gravity level) is nearly zero. Small disturbances decrease 0.5 s after release. Neglecting these disturbances, the duration of 10 s with a reduced gravity level of 10^{-4}–10^{-3} g_0 is the longest achieved worldwide in terms of both quantity and quality. The acceleration in the braking zone is less than 10 g_0 in the z-axis direction.

The duration for which microgravity conditions were achieved −10 s – was too short to observe the tube quenching phenomenon in the various boiling regimes, which included film boiling, transition boiling, and nucleate boiling. In the present study, we decided to focus on experiments dealing with the influence of gravity in the neighborhood of the important solid–liquid contact line (quench front) in the quenching phenomenon.

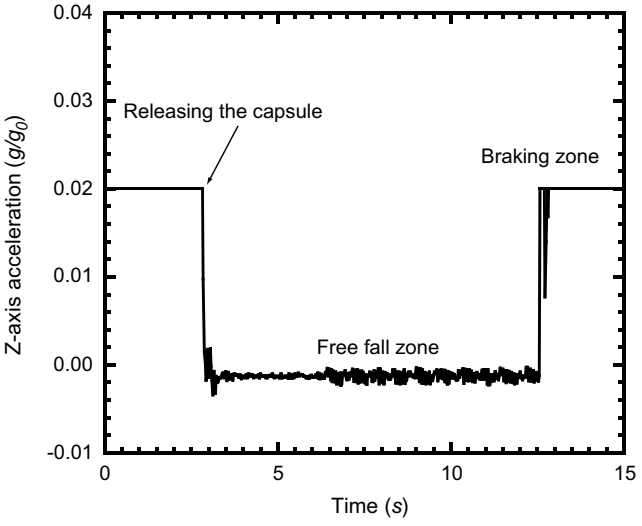

Fig. 3. An example of gravitational acceleration in the JAMIC drop shaft.

2.3. Calibration of thin gold film

For evaluating the inner wall temperature [7], the electric resistance R is directly calculated from $R = (V/V_0)R_0$ by using a simple circuit as shown in Fig. 4, where R_0 is the value of the standard resistance connected in series and V and V_0 are the voltages across the resistances R

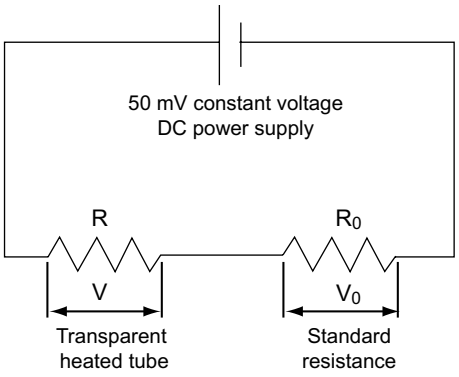

Fig. 4. Electric circuit for the measurement of the resistance of the transparent heated tube.

and R_0, respectively. In the present study, in order to determine the relation between the resistance R and temperature T_w, a very low electric voltage (50 m VDC) is applied, so as not to increase the inner wall temperature; here, the temperature of the film is assumed to be the same as that of the thermostatic bath with the submerged tube. In this test, these data was measured to an accuracy of 6.5 digits. As an example of the calibration test, the inner wall temperature averaged over the entire temperature measurement length of the tube, T_w, was found to be proportional to the resistance of the thin gold film, R, as shown in Fig. 5. The temperature coefficient of the film determined from the figure is 73.0834 (K/Ω), and this gradient remained almost constant for the duration of the experiment. However, the value of the y-intercept was required to be fixed for every experiment. Accordingly, this calibration test was conducted before and after each experiment, and the calibration curve was determined from the average of these tests.

2.4. Measurement of mass velocity

In the present study, the Dewar vessel of the LN_2 tank is made of pyrex glass, and it can be used to observe LN_2 behavior during the experiment. Therefore, the mass velocity can be derived by measuring the displacement of the LN_2 surface in the tank. Since the JAMIC capsule mounted with the experimental apparatus is sealed, we can also determine the amount of evaporation of liquid nitrogen in the microgravity experiments from capsule pressure measurements. Additionally, the method of measuring mass velocity using the pressure difference between the inlet and outlet of the test section [6] is compared with the abovementioned methods, and the average mass velocity is determined. Fig. 6 shows the average mass velocity G vs. GN_2 pressure based on these measurement methods under terrestrial and microgravity conditions. The results indicate that the average mass velocity measurement of cryogenic fluids using our experimental apparatus is a linear function of the GN_2 pressure under different gravity conditions.

2.5. Experimental procedure

The experiments were conducted using LN_2 at mass velocity $G = 100$–$300\ \mathrm{kg/m^2\,s}$. This mass velocity range is nearly equal to the velocity of fuel transfer in the re-ignition of the rocket engine on orbit. An air compressor is employed for controlling the system pressure changed by natural evaporation of LN_2 before the microgravity experiment started. This compressor is operated when the pressure exceeds 0.11 MPa, and is stopped when it becomes less than 0.10 MPa. The amount of LN_2 used in the microgravity experiments did not exceed 500 ml in accordance with JAMIC restrictions.

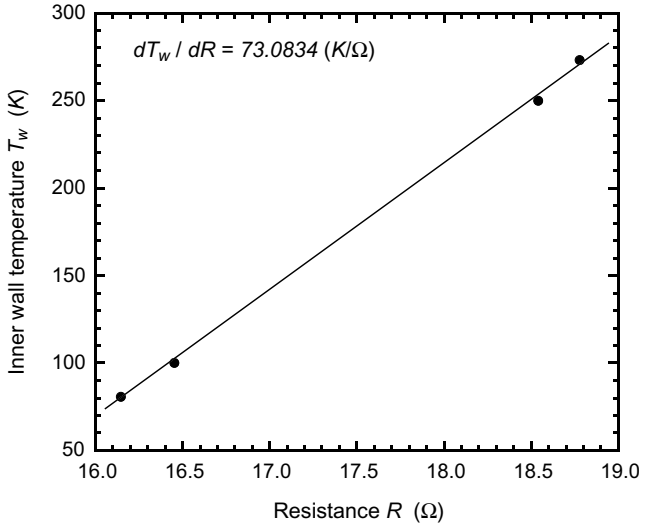

Fig. 5. Calibration test for the relation between the temperature and resistance of the thin gold film coated on the inner wall of the tube in the cryogenic temperature region.

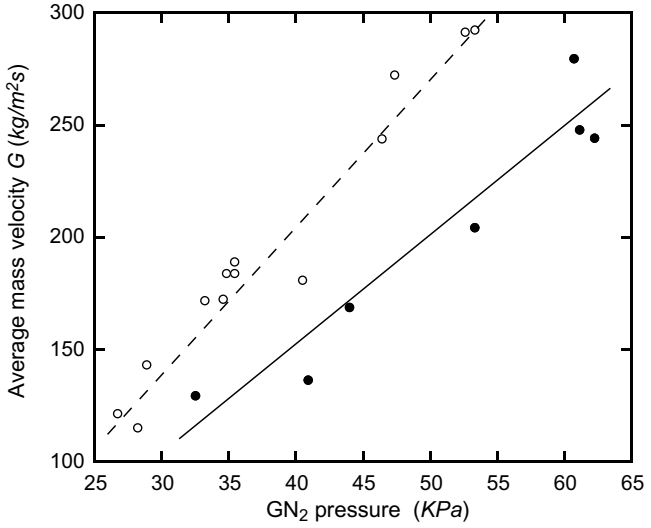

Fig. 6. Measured LN_2 mass velocity as a function of the average GN_2 pressure under terrestrial and microgravity conditions (•, μg; ○, $1g$).

Initially, GN_2, whose pressure is controlled by a pressure regulator, expels the LN_2 from its tank to the test section. The start signal runs to get the quench front in microgravity a few seconds before microgravity commences. LN_2 passes through the tube from its bottom, and the flow direction is against gravity under 1*g*. The initial tube temperature is maintained at room temperature (about 300 K). The flow behavior in the tube and LN_2 tank is observed by CCD cameras. The fluid temperatures at the inlet and outlet of the test section and the outer wall temperature of the tube are measured with K-type thermocouples. The standard estimation errors of the thermocouples are within ± 0.2 K.

The acquired data and photographs of flow behavior in microgravity are synchronized with the aid of a microgravity starting signal from the support system installed at JAMIC. A data logger with seven isolated channels is used for the measuring voltages, which include four thermocouples, the voltage of the thin gold film, the standard resistance, and the microgravity signal, with a sampling frequency of 10 Hz.

3. Results and discussion

3.1. Heat transfer characteristics

Fig. 7 shows a comparison between the inner wall temperature histories for the μg and 1*g* experiments under $G = 170$ kg/m^2 s. The quenching time in which the inner wall temperature changed from 300 K to the LN_2 temperature (77.3 K) under microgravity conditions was shorter than that under terrestrial conditions; the quenching time in the case of 170 kg/m^{2}s was 13.0 s under 1*g* and 11.5 s under μg. In the case of this figure, the cooling rate appears to be higher at reduced gravity. For a more detailed consideration, a comparison of the quenching time as a function of the mass velocity for all the 1*g* and μg experiments conducted in this study are shown in Fig. 8. The quenching time under microgravity conditions was a maximum of about 20% shorter than that under terrestrial conditions; the difference decreases with increasing average mass velocity. In our experimental conditions, we observe that the influence of gravity almost disappears when the average mass velocity exceeds 250 kg/m^2 s.

Next, we consider heat transfer characteristics such as heat flux under microgravity conditions. The heat flux q_w and heat transfer coefficient α_w at the inner wall of the tube are given by

$$q_w = -\lambda \frac{1}{r} \frac{\partial T}{\partial r},$$

and

$$\alpha_w = \frac{q_w}{T_w - T_l}$$

where λ, r, and T_w are the thermal conductivity of the tube, coordinate of radial direction, and inner wall temperature, respectively. Notice that T_w, q_w and α_w are averaged value over the entire temperature measurement length of the tube. The liquid temperature T_l is calculated as the average of the inlet and outlet fluid temperatures.

The boiling curve is shown in Fig. 9. The pattern of the boiling curve under μg is similar to that under 1*g*, as shown in Fig. 9. However, from this figure, we observe that q_{max} and q_{min} under μg are about 1.4 times and 1.2 times larger than those under 1*g*, respectively. Furthermore, $q_{max} - q_{min}$ under μg is about 0.8 times smaller than that under 1*g*. This shows that the required heat quantity in transition boiling under μg is less than that under 1*g*, indicating that LN_2 came in contact with the inner wall at an earlier time. In

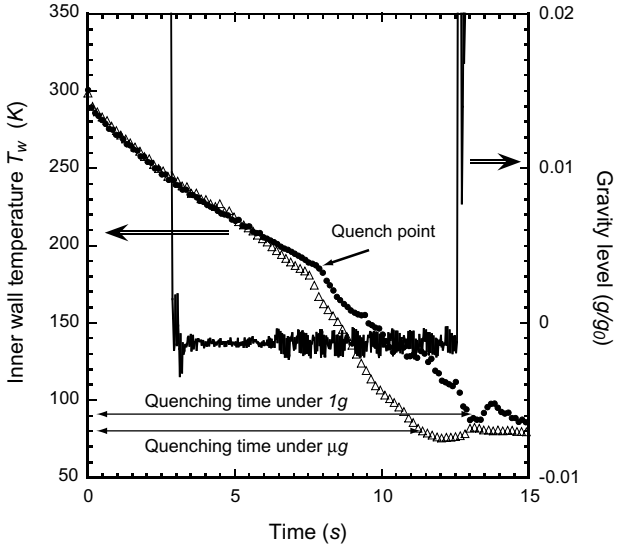

Fig. 7. Inner wall temperature histories for average mass velocity 170 kg/m^2 s (•, 1*g*, △, μg).

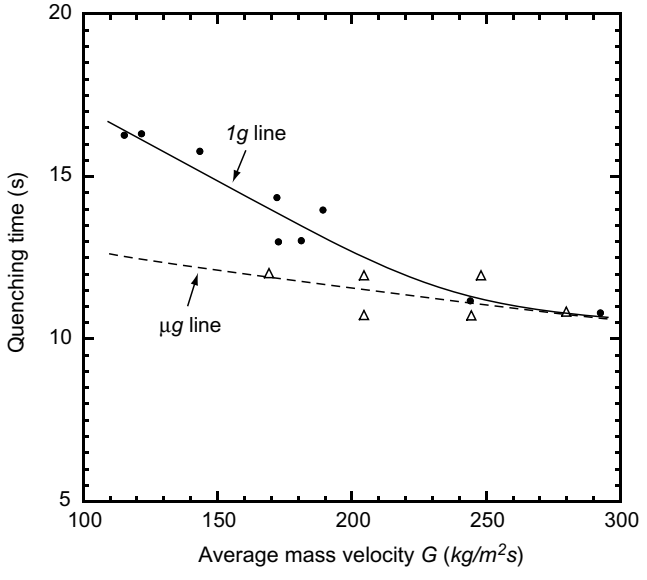

Fig. 8. Variation of the quenching time with average mass velocity for all the tests (•, 1*g*, △, μg).

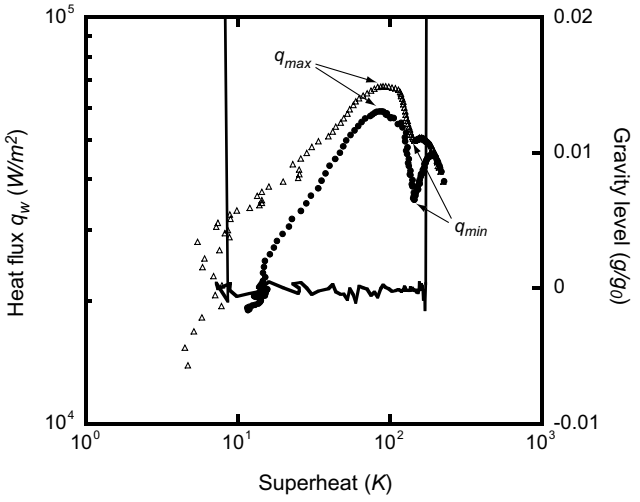

Fig. 9. Heat flux versus wall superheat for average mass velocity 244 kg/m^2 s (•, 1g, △, μg; –, gravity level).

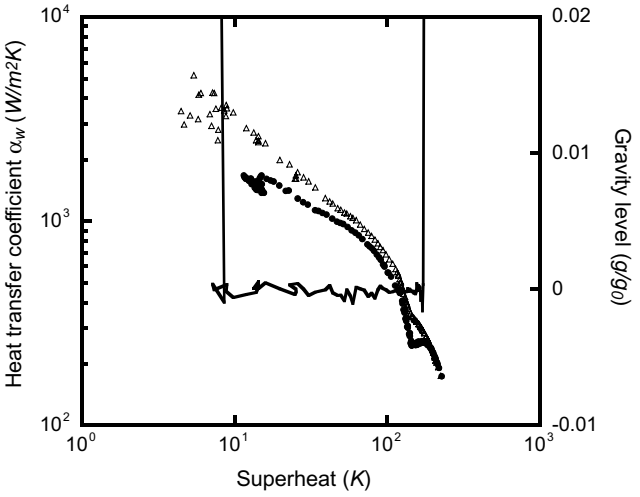

Fig. 10. Heat transfer coefficients vs. wall superheat for average mass velocity 244 kg/m^2 s (•, 1g; △, μg; –, gravity level).

fact, the integration values of the heat flux during the quenching in 1g and μg were almost the same. The relation between superheat and the heat transfer coefficient at the inner wall of the tube is shown in Fig. 10. It is evident that heat transfer coefficients under μg are larger than those under 1g, and the difference between the heat transfer coefficients increased as the superheat decreased.

Now, let us consider the influence of gravity in the relation between heat flux and mass velocity. Fig. 11 shows the maximum heat flux q_{max} under 1g and μg. The difference between q_{max} under microgravity and terrestrial conditions does not change with the increase in mass velocity; however, the q_{max} under microgravity conditions is larger than that under terrestrial conditions. This result is corresponding to a short quenching time under μg, as shown in Fig. 7. From the above results, it is evident that the heat transfer in cryogenic forced convective boiling in a low mass velocity region under μg is more promoted than that under 1g.

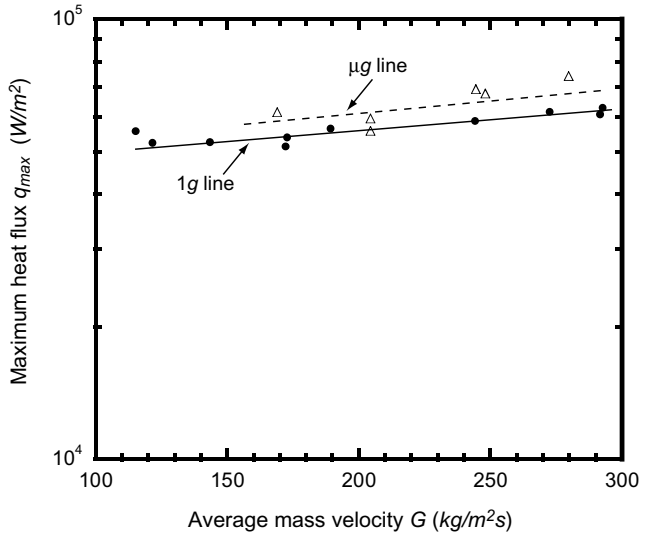

Fig. 11. Variation of the maximum heat flux with average mass velocity (•, 1g; △, μg).

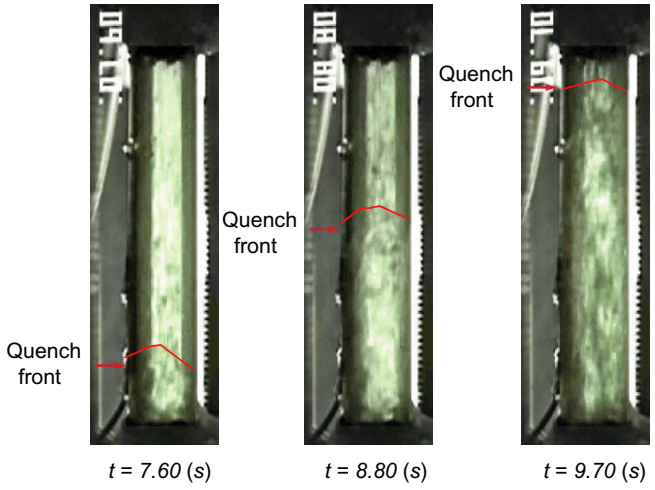

Fig. 12. Three single frames showing downstream motion of the quench front (average mass velocity 169.0 kg/m^2 s, under μg).

3.2. Quench front velocity

The present experiments were aimed at obtaining temperature measurements and visual recordings simultaneously, but clear photographs could not be captured, because of the moisture caused by the boiling of LN_2 in the tube. However, we successfully observed the advancing quench front, as shown in Fig. 12. The advancing speed of the quench front was determined from these photographs.

The relation between the quench front velocity and average mass velocity is shown in Fig. 13. The quench front velocity under μg increases up to 20% from that under 1g, and the difference between the quench front velocity under 1g and μg decreases with an increase in the average mass velocity. Here, we introduce the dimensionless quantity u_q/u_I; the relation between this quantity and the

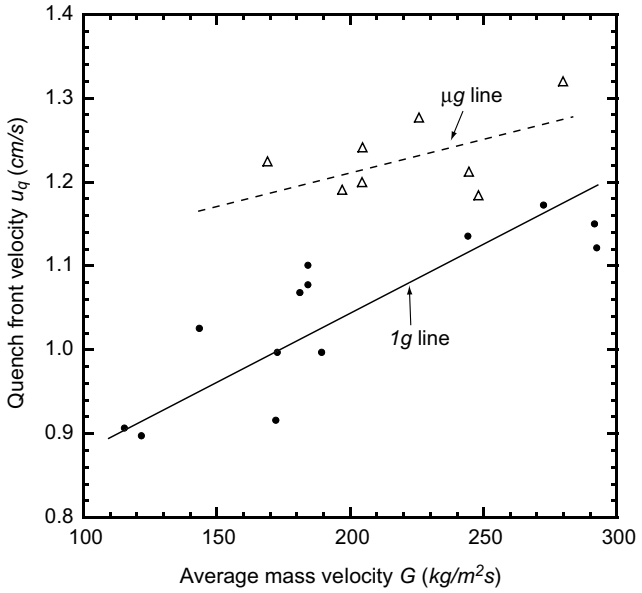

Fig. 13. Variation of the quench front speed with average mass velocity (•, 1g; △, μg).

average mass velocity is shown in Fig. 14. From this figure, it is evident that the dimensionless velocity under microgravity conditions increases up to 20% from that under 1g, and the difference between this velocity under 1g and μg decreases with increasing mass velocity. This implies that the gravity force affects the quench front velocity under 1g and thus the quench front velocity under 1g becomes smaller than that under μg. This increasing trend of the quench front velocity coincides with the increasing trend of the heat transfer and the decreasing trend of the quenching time under microgravity, as shown in Figs. 11 and 13, implying that they were closely related. However, it is still unclear as to why the quench front velocity is faster under microgravity conditions than under terrestrial conditions, which is an important issue that remains to be addressed. At present, it is assumed to be due to the notable wettability of liquid on the quench front (gas–liquid contact line) in microgravity. The relation between the quench front velocity and the gravity force is an issue that requires detailed study in the future.

Let us consider the energy balance equation at any position of z from the bottom of the tube, since the difference in the quench front velocity affects the heat transfer of the cryogenic flow boiling [9]

$$(\rho c_p)_w \delta_w \frac{\partial T_w}{\partial t} = \kappa_w \delta_w \left(\frac{\partial^2 T_w}{\partial z^2} + \frac{\partial^2 T_w}{\partial x^2} \right) - q_w + q_G \delta_w, \qquad (1)$$

where the generated heat q_G may be regarded as 0 in our experiment. Assuming that the tube is flat plate in this equation because the tube wall is thin, x is the coordinate of wall thickness direction.

Assuming that the quench front velocity is constant, the temperature distribution in the z-direction does not change its form when moving to an upper position. Thus, the first term on the right-hand side of Eq. (1) can be reduced to the following:

$$\frac{\partial^2 T_w}{\partial z^2} = \frac{1}{u_q^2} \frac{\partial^2 T_w}{\partial t^2}. \qquad (2)$$

Using Eq. (2) and $q_G = 0$, Eq. (1) becomes

$$q_w = \delta_w \left(-(\rho c_p)_w \frac{\partial T_w}{\partial t} + \frac{\kappa_w}{u_q^2} \frac{\partial^2 T_w}{\partial t^2} + \frac{\partial^2 T_w}{\partial x^2} \right). \qquad (3)$$

The variations in the temperature of the inner wall of the tube with time are plotted in Fig. 15. As seen in this figure, the $\partial T_w/\partial t$ (the averaged value over the entire temperature measurement length) gradients between 6 and 6.5 s, which

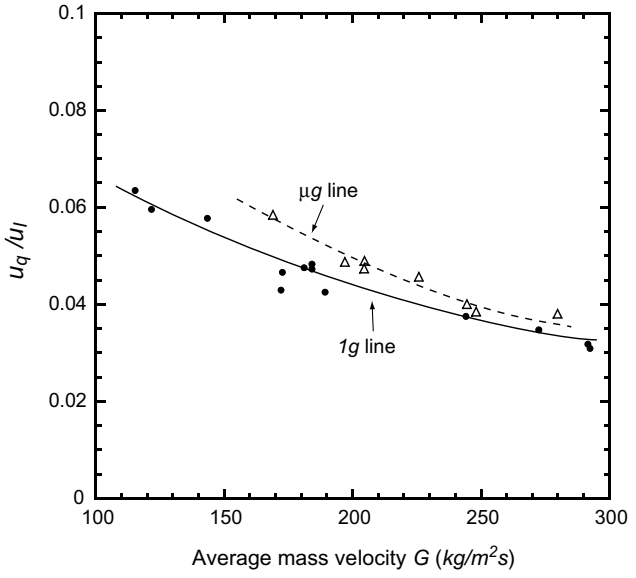

Fig. 14. Variation of the non-dimensional quench velocity with average mass velocity (•, 1g; △, μg).

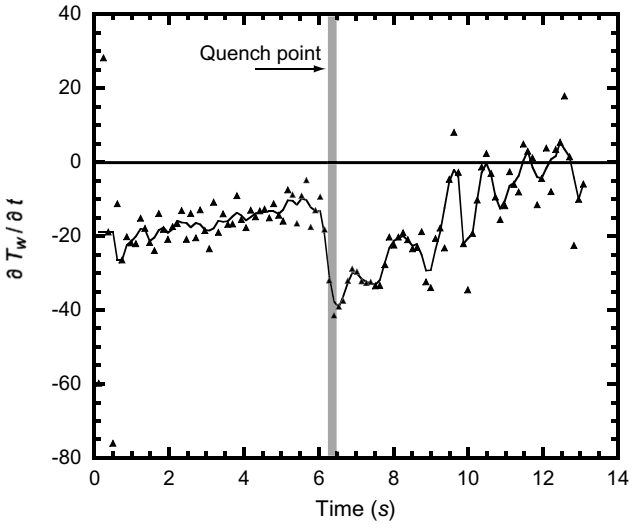

Fig. 15. Typical $\partial T_w/\partial t$ histories (average mass velocity 240 kg/m^2 s, under μg).

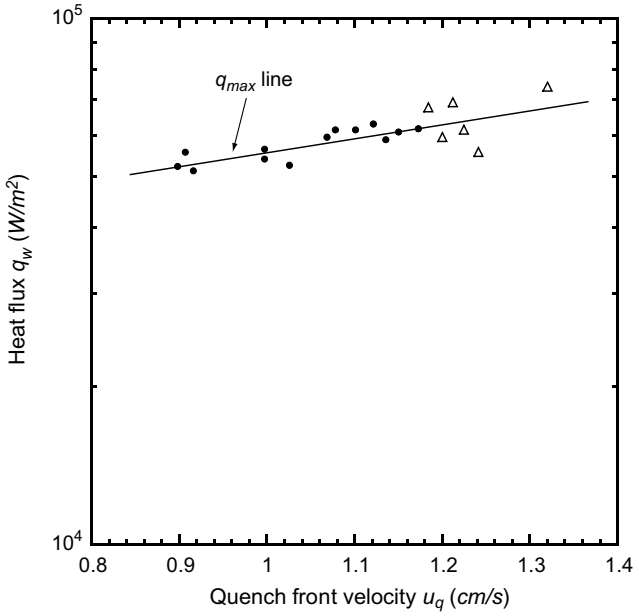

Fig. 16. Maximum heat flux versus quench front velocity for all the tests (•, 1g; △, μg).

coincide with the passing of the quench front in the tube, have a large negative value and exert a dominant effect on q_w. Due to the negative $\partial^2 T_w/\partial t^2$, q_w increases with increasing u_q in Eq. (3). This explains why q_{max} under microgravity, which commences with the passing of the quench front in the tube, is larger than that under 1g, as shown in Fig. 11. The relationship between the maximum heat flux and quench front velocity is shown in Fig. 16. The maximum heat flux increases as an exponential function of the quench front velocity and is independent of the gravity level. It was concluded from these results that the increase in the heat transfer under microgravity conditions was caused by the increase in the quench front velocity.

4. Conclusion

In this paper, heat transfer during tube quenching by a cryogenic fluid under microgravity conditions was investigated. The microgravity experiments were conducted at JAMIC using LN_2 as a test fluid, and a transparent heated tube was employed for observing fluid behavior and measuring heat transfer during tube quenching. These experiments were aimed at understanding the relation between the flow behavior and thermal characteristics during tube quenching by a cryogenic fluid under microgravity conditions, and they were conducted in a low mass velocity region (100–300 kg/m^2 s) that is easily influenced by gravity. Simultaneous measurements of the thermal characteristics and quench front velocity were successfully carried out, and the results are summarized as follows:

(1) The heat transfer and quench front velocity increase in microgravity.
(2) The heat transfer and quench front velocity under microgravity conditions increase up to 20% from those under 1g, and the difference in the heat transfer characteristics under 1g and μg decreases with increasing mass velocity.
(3) The relationship between the increase rates of the heat transfer and quench front velocity is illustrated by considering the heat balance equation; further, the maximum heat flux increases as an exponential function of the quench front velocity and is independent of gravity.

It is concluded from these results that the increase in the heat transfer under microgravity conditions is caused by the increase in the quench front velocity.

Acknowledgements

The authors express their appreciation to Professor B.N. Antar from the University of Tennessee Space Institute for his valuable comments. The author, O. Kawanami, is extremely grateful for the assistance provided by the JAMIC staff in the microgravity experiments.

References

[1] T. Himeno, T. Watanabe, A. Konno, Numerical analysis of two-phase flow behavior in a liquid propellant tank, AIAA 99–2177, 1999.
[2] T. Toru, S. Nakasuka, Fuel station-based transportation network as a future space infrastructure, Preprints of 43rd Congress of IAF, IAA-92-0168, 1992.
[3] L.J. Hastings, S.P. Tucker, C.F. Huffaker, CFM technology needs for future space transportation systems, in: AIAA/NASA/OAI Conf. on Advanced SEI Technologies, AIAA 91–3474, 1991.
[4] J. Straub, Boiling heat transfer and bubble dynamics in microgravity, in: J.P. Hartnett, T.F. Irvine, Jr., Y.I. Cho, G.A. Greene (Eds.), Advances in Heat Transfer, vol. 35, Academic Press, 2001, pp. 57–172.
[5] H. Ohta, Microgravity heat transfer in flow boiling, in: J.P. Hartnett, T.F. Irvine, Jr., Y.I. Cho, G.A. Greene (Eds.), Advances in Heat Transfer, vol. 37, Academic Press, 2003, pp. 1–74.
[6] B.N. Antar, F.G. Collins, Flow boilling during quench in low gravity environment, Microgravity Sci. Technol. X/3 (1997) 118–128.
[7] H. Ohta, K. Inoue, Y. Yamada, S. Yoshida, H. Fujiyama, S. Ishikura, Microgravity flow boiling in a transparent tube, in: Proceedings of the 4th ASME/JAME Thermal Eng. Conf. (1995) pp. 547–554.
[8] Japan Microgravity Center and Japan Space Utilization Promotion Center, Japan Microgravity Center user's guide, 1999.
[9] T. Ueda, Gas and liquid two-phase flow, Yokendo (1981) 329–335 (in Japanese).